Both liver-X receptor (LXR) isoforms control energy expenditure by regulating Brown Adipose Tissue activity

Marion Korach-André[a,1], Amena Archer[a,1], Rodrigo P. Barros[b], Paolo Parini[a,c], and Jan-Åke Gustafsson[a,b,1]

[a]Department of Biosciences and Nutrition at NOVUM, Karolinska Institutet, 14183 Huddinge, Sweden; [b]Center for Nuclear Receptors and Cell Signaling, Department of Cell Biology and Biochemistry, University of Houston, TX 77204; and [c]Division of Clinical Chemistry, Department of Laboratory Medicine, Karolinska Institutet at Karolinska University Hospital, 14186, Huddinge, Sweden

Contributed by Jan-Åke Gustafsson, November 30, 2010 (sent for review November 15, 2010)

Brown adipocytes are multilocular lipid storage cells that play a crucial role in nonshivering thermogenesis. Uncoupling protein 1 (UCP1) is a unique feature of brown fat cells that allows heat generation on sympathetic nervous system stimulation. As conventional transcriptional factors that are activated in various signaling pathways, liver-X receptors (LXRs) play important roles in many physiological processes. The role of LXRs in the regulation of energy homeostasis remains unclear, however. Female WT, LXRαβ$^{-/-}$, LXRα$^{-/-}$, and LXRβ$^{-/-}$ mice were fed with either a normal diet (ND) or a high-carbohydrate diet (HCD) supplemented with or without GW3965-LXR agonist. LXRαβ$^{-/-}$ mice exhibited higher energy expenditure (EE) as well as higher UCP1 expression in brown adipose tissue (BAT) compared with WT mice on the HCD. In addition, long-term treatment of WT mice with GW3965 showed lower EE at thermoneutrality (30 °C) and lower *Ucp1* expression level in BAT. Furthermore, H&E staining of the BAT of LXRαβ$^{-/-}$ mice exhibited decreased lipid droplet size compared with WT mice on the HCD associated with a more intense UCP1-positive reaction. Quantification of triglyceride (TG) content in BAT showed lower TG accumulation in LXRβ$^{-/-}$ mice compared with WT mice. Surprisingly, GW3965 treatment increased TG content (twofold) in the BAT of WT and LXRα$^{-/-}$ mice but not in LXRβ$^{-/-}$ mice. Furthermore, glucose transporter (GLUT4) in the BAT of LXRα$^{-/-}$ and LXRβ$^{-/-}$ mice was sixfold and fourfold increased, respectively, compared with WT mice on the ND. These findings suggest that LXRα as well as LXRβ could play a crucial role in the regulation of energy homeostasis in female mice and may be a potential target for the treatment of obesity and energy regulation.

Obesity has become a major health issue in Western and developing countries and is a crucial factor in the development of common associated metabolic diseases. Recently, brown adipose tissue (BAT) thermogenesis was proposed as a mechanism not only for regulating body temperature but to protect against obesity and the development of insulin resistance (1–4). The concept that BAT is a thermogenic tissue initially came from morphological changes in the tissue when animals were exposed to cold (5). BAT thermogenesis burns off excess calories during positive energy balance to maintain energy homeostasis. Diet-induced thermogenesis was supported by evidence that cold sensitivity and obesity phenotypes in *ob*/*ob* mice were associated with defective BAT nonshivering thermogenesis (6, 7). It is now well established that energy expenditure (EE) increases as a function of body mass in humans and, accordingly, that severe obesity is associated with an increase in EE (8–10).

Although white adipose tissue (WAT) is the main adipose tissue, BAT is present in small mammals and has recently been shown to be present in adult humans as well (2, 11, 12). BAT, in which glucose is an important fuel in vivo, is a target tissue for insulin action, especially during late fetal development when insulin promotes adipogenic and thermogenic differentiation (13). BAT expresses high levels of peroxisome proliferator-activated receptor γ (PPARγ) (14) as well as liver-X receptors (LXRs) (15) and, consequently, is a target for nuclear receptor agonists. Although LXR function has been elucidated in detail with respect to cholesterol and lipid metabolism, recent findings have indicated that LXR is also an important modulator of glucose and water homeostasis as well as energy regulation (16–21).

LXRαβ$^{-/-}$ and LXRβ$^{-/-}$ mice have been shown by our group and others to be resistant to high-fat diet-induced obesity (17, 18, 22). Several explanations have been proposed, such as increased EE or a resistance to insulin-induced lipid storage (17, 18). To our knowledge, however, the effect of deletion/activation of LXRs on glucose and lipid metabolism in brown adipocytes has not been explored in female C57BL/6 mice. In the current study WT, LXRαβ$^{-/-}$, LXRα$^{-/-}$, and LXRβ$^{-/-}$ mice were challenged with either a normal diet (ND) or a high-carbohydrate diet (HCD) supplemented with or without LXR synthetic agonist GW3965 for 3 wk. Our results indicate that LXRα and LXRβ control EE in the BAT. Indeed, long-term LXR activation by agonist GW3965 is associated with reduced EE at thermoneutrality (30 °C) in female mice. In addition, we observed a sixfold and fourfold increase of GLUT4 expression in the BAT of LXRα$^{-/-}$ and LXRβ$^{-/-}$ mice, respectively, compared with WT mice, further supporting the idea of a sharing responsibility of LXRα and LXRβ in the regulation of BAT metabolism.

Results

EE Is Increased in LXRαβ$^{-/-}$ Mice and Reduced in WT Mice Treated with LXR Agonist GW3965 Compared with WT Mice on the HCD. Ten-week-old female C57BL/6 mice were fed with either the ND or HCD for 3 wk. Body weight (BW) was similar between groups on both diets (Fig. 1*A*, *Left*). Nevertheless, a significantly decreased BW was observed in WT mice after GW3965 treatment (Fig. 1*A*, *Left*) compared with the HCD. Caloric intake, measured daily over a 1-wk period, was lower in LXRαβ$^{-/-}$ mice on both diets compared with WT mice (Fig. 1*A*, *Right*). Interestingly, GW3965 treatment together with the HCD significantly reduced food intake (FI) in WT mice compared with the HCD alone. LXRαβ$^{-/-}$ mice have been shown to be resistant to diet-induced obesity (17, 18). Because resistance to diet-induced obesity can be the consequence of an increase of EE, oxygen consumption and carbon dioxide release were registered in WT and LXRαβ$^{-/-}$ mice after 3 wk on the HCD for 48 h in temperature-controlled (23 °C) individual chambers. Cage temperature was raised to 30 °C for 3 h to measure acute thermoneutral metabolism response. EE was significantly higher in LXRαβ$^{-/-}$ mice compared with WT animals during the dark period, but only a trend toward increased EE was observed during the light period at 23 °C and 30 °C (Fig. 1*B*). More

Author contributions: M.K.-A. designed research; M.K.-A. and A.A. performed research; P.P. contributed new reagents/analytic tools; M.K.-A., A.A., R.P.B., and J.-Å.G. analyzed data; and M.K.-A. and J.-Å.G. wrote the paper.

The authors declare no conflict of interest.

[1]To whom correspondence may be addressed. E-mail: marion.korach-andre@ki.se, amena.archer@ki.se, or jgustafs@central.uh.edu.

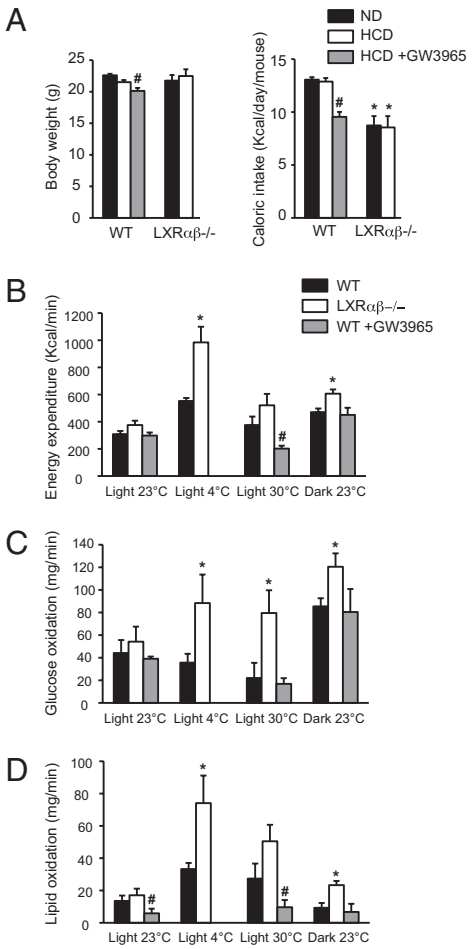

Fig. 1. EE is increased in LXRαβ$^{-/-}$ mice and reduced in WT mice treated with LXR agonist GW3965 compared with WT mice on the HCD. (*A*) BW and caloric intake after 3 wk of the ND (black bar) or the HCD (open bar) in WT and LXRαβ$^{-/-}$ mice as well as after the HCD together with GW3965 (gray bar) in WT mice only. Mean value of EE (44) (*B*), glucose oxidation (*C*), and fat oxidation (*D*) under different physiological conditions (i.e., 12-h light/12-h dark period at 23 °C, 3-h light period at 4 °C, and 3-h light period at 30 °C in WT (white bar), LXRαβ$^{-/-}$ (black bar), and WT + GW3965 (gray bar) mice (one-way ANOVA, n = 5–8 animals per group; $^{*}P < 0.05$ in LXR KO vs. WT mice; $^{\#}P < 0.05$ in HCD vs. HCD + GW3965).

importantly, when synthetic LXR ligand (GW3965) was added to the diet for 3 wk, EE was significantly reduced compared with WT mice fed the HCD at thermoneutrality (30 °C) (Fig. 1*B*). Cold exposure is known to activate the sympathetic nervous system, and BAT thermogenesis and uncoupling protein 1 (UCP1) expression are increased during chronic cold exposure to produce heat (23). When cage temperature was lowered to 4 °C, LXRαβ$^{-/-}$ mice showed a significantly higher EE compared with WT mice. Substrate (glucose and lipid) oxidation was calculated from volume of carbon dioxide (VCO_2) and volume of oxygen (VO_2) (Fig. 1 *C* and *D*). LXRαβ$^{-/-}$ mice showed higher glucose and lipid oxidation under all metabolic conditions except during the light period at 23 °C compared with WT mice (Fig. 1 *C* and *D*). WT mice treated with GW3965 for 3 wk showed lower lipid oxidation during the light period at 23 °C and 30 °C compared with WT mice (Fig. 1*D*).

LXRαβ$^{-/-}$ Mice Showed Smaller Lipid Droplets and Higher UCP1-Positive Reaction in BAT Compared with WT Mice on the HCD. Because FI is correlated to nonshivering thermogenesis, we investigated brown adipose histology of WT and LXRαβ$^{-/-}$ mice. H&E staining of the BAT showed no differences in lipid droplet sizes between genotypes on the ND (Fig. 2A). After HCD challenge, however, smaller lipid droplets were observed in the BAT of LXRαβ$^{-/-}$ mice compared with WT mice (Fig. 2*A*). To explore further why lipid droplets were smaller and EE was higher in LXRαβ$^{-/-}$ mice compared with WT mice, we stained BAT for UCP1, the main protein involved in nonshivering thermogenesis. A varying amount of BAT was present in all sections, with a more intense UCP1-positive reaction in the BAT of LXRαβ$^{-/-}$ mice on the ND and HCD (Fig. 2*B*) compared with WT animals.

Increased Subcutaneous Leptin Expression and Gonadal Fat UCP1 Expression in LXRα$^{-/-}$ Mice. Most studies converge to say that total BAT activity is inversely associated with adiposity, suggesting that increasing BAT mass and/or activity may be an aim in pharmaceutical intervention against obesity (2, 11). Recently, Wang et al. (20) suggested that LXRα but not LXRβ regulates the *Ucp1* gene and brown fat phenotype. We thus measured by MRI whole-body fat content and distribution in WT, LXRα$^{-/-}$, and LXRβ$^{-/-}$ mice on the ND to avoid diet-induced thermogenesis phenomena. No differences existed in BW between groups (18.6 ± 0.8 vs. 19.2 ± 0.4 vs. 18.7 ± 0.6 in WT, LXRα$^{-/-}$, and LXRβ$^{-/-}$ mice, respectively). Furthermore, no differences were observed between LXRα$^{-/-}$ and WT mice regarding total fat storage (TF)/BW ratio, whereas a significant decrease was observed in LXRβ$^{-/-}$ mice (Fig. 3*A*, *Left*). Visceral (VS)/BW and subcutaneous (SC)/BW ratios showed no statistical differences between groups, but a trend toward decreased VS/BW ratio was observed in LXRβ$^{-/-}$ mice as opposed to a trend toward decreased SC/BW ratio in LXRα$^{-/-}$ mice compared with WT mice (Fig. 3*A*, *Right*). Surprisingly, expression of *Leptin* gene was 2.5-fold higher in SC fat of LXRα$^{-/-}$ mice compared with WT mice, whereas no differences were observed between groups in gonadal fat. Recent reports have shown that ectopic *Ucp1* expression in WAT (24) can appear because of differentiation of white fat cells into brown fat cells in the WAT (4, 25). A 10-fold increase associated with a fivefold decrease of Ucp1 expression was observed in gonadal vs. SC fat, respectively, in LXRα$^{-/-}$ mice compared with WT mice

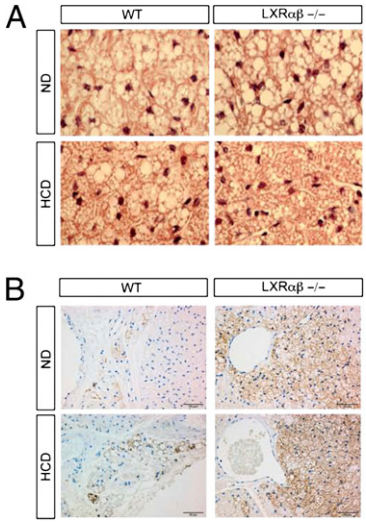

Fig. 2. LXRαβ$^{-/-}$ mice showed smaller lipid droplets and higher UCP1-positive reaction in brown adipose compared with WT mice on HCD. One representative histological analysis of H&E-stained sections of BAT (*A*) and immunofluorescence detection of UCP1 (*B*) in the BAT of WT and LXRαβ$^{-/-}$ mice on the ND and HCD, respectively (n = 7 animals per group).

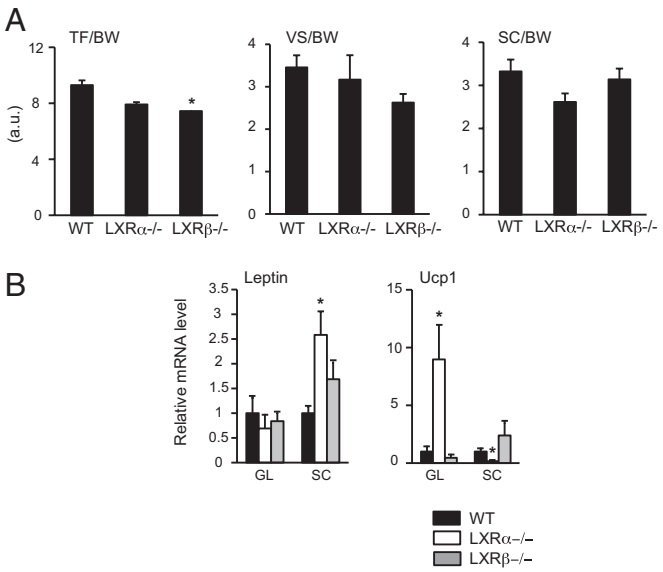

Fig. 3. Fat distribution measured by MRI and different gene expression between SC and gonadal fat pad in LXRα$^{-/-}$ mice. TF/BW, VF/BW, and SC/BW (*A*) and gonadal (GL) and SC (*B*) mRNA expression levels of leptin and Ucp1 genes in WT (black bar), LXRα$^{-/-}$ (white bar), and LXRβ$^{-/-}$ (gray bar) mice, respectively, on the ND. Relative fold changes in expression levels were compared with WT mice, in which the expression was set to 1.0 and normalized to transcription factor IID (TFIID) expression (one-way ANOVA, $n = 7$ animals per group;*$P < 0.05$ in LXR KO vs. WT mice).

(Fig. 3*B*). No significant differences were observed in LXRβ$^{-/-}$ mice compared with WT mice.

Decreased UCP1 Expression in the BAT of WT, LXRα$^{-/-}$, and LXRβ$^{-/-}$ Mice Treated with LXR Ligand GW3965. For a more exhaustive investigation of LXR regulation of UCP1, staining for UCP1 and mRNA expression level of *Ucp1* and UCP1 protein expression in BAT were analyzed in LXRα$^{-/-}$, LXRβ$^{-/-}$, and WT mice treated or not treated with GW3965 for 3 wk. As observed in LXRαβ$^{-/-}$ mice in Fig. 2*B*, a varying amount of BAT was present in all sections, with a possibly less intense UCP1-positive reaction in the BAT of LXRβ$^{-/-}$ mice compared with LXRα$^{-/-}$ and WT mice (Fig. 4*A*). Expression of *Ucp1* was 10-fold and threefold higher in LXRα$^{-/-}$ and LXRβ$^{-/-}$ mice, respectively, compared with WT mice (Fig. 4*B*). More importantly, mRNA level of *Ucp1* was significantly reduced in the BAT of WT mice treated with GW3965 by gavage for 3 d (Fig. 4*C*). UCP1 quantification by Western blot analysis showed a 3.8-fold increase of UCP1 in LXRα$^{-/-}$ mice compared with WT mice. Chronic LXR agonist treatment for 3 wk abolished UCP1 expression in WT, LXRα$^{-/-}$, and LXRβ$^{-/-}$ mice (Fig. 4*D*). We can thus conclude that LXRα as well as LXRβ regulates UCP1 expression in BAT.

Regulation of GLUT4 by LXRs in BAT. Whereas it is has been demonstrated that an increase in free fatty acid level is a necessary step for activation of UCP1 [reviewed by Cannon et al. (26)], once activated, the cells burn both carbohydrates and lipids. Two facilitative glucose transporter isoforms, GLUT1 and GLUT4, have been identified in BAT (27, 28). GLUT4, the insulin-sensitive transporter, is likely responsible for most of the glucose taken up by the tissue (27, 28). We thus investigated glucose transporter (Glut4) expression in the BAT of WT, LXRα$^{-/-}$, and LXRβ$^{-/-}$ mice treated or not treated with GW3965. Expression of *Glut4* as well as *Irs2* (but not *Irs1*) was increased in LXRα$^{-/-}$ mice compared with WT mice (Fig. 5A) in line with the improved glucose disappearance from the blood following an i.p. insulin dose ob-

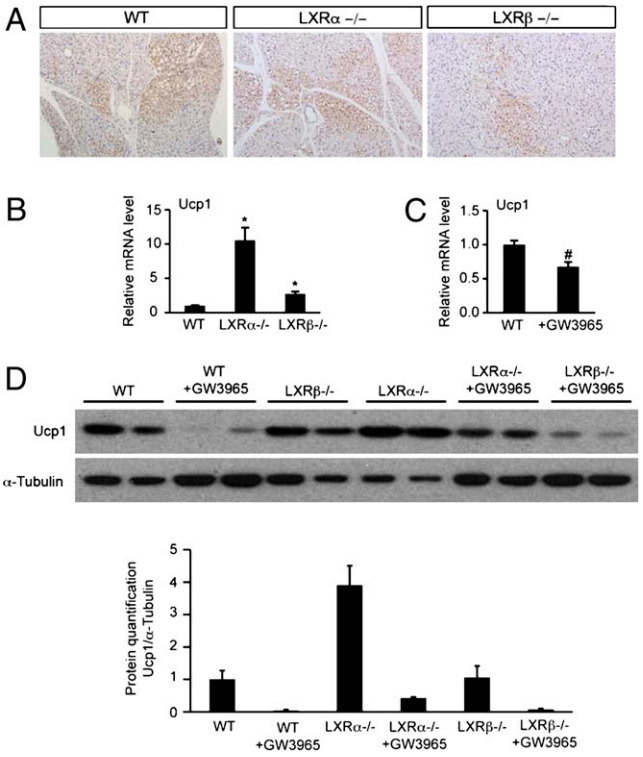

Fig. 4. UCP1 expression is increased in the BAT of LXRα$^{-/-}$ mice compared with WT mice on the ND and is decreased in the BAT of WT, LXRα$^{-/-}$, and LXRβ$^{-/-}$ mice treated with the LXR ligand GW3965. (*A*) One representative immunofluorescence investigation of UCP1 in the BAT of WT, LXRα$^{-/-}$, and LXRβ$^{-/-}$ mice on the ND. mRNA expression levels of UCP1 in the BAT of WT, LXRα$^{-/-}$, and LXRβ$^{-/-}$ mice on the ND (*B*) and of WT ± GW3965-treated mice (*C*). Relative fold changes in expression levels were compared with the WT mice in the ND group, in which the expression was set to 1.0 and normalized to TFIID expression (one-way ANOVA, $n = 5$–7 animals per group; *$P < 0.05$ in LXR KO vs. WT mice; #$P < 0.05$ in ND vs. ND + GW3965). (*D*) Detection of UCP1 expression in BAT by Western blotting in WT, LXRα$^{-/-}$, and LXRβ$^{-/-}$ mice on the ND ± GW3965-fed mice.

served in the LXRα$^{-/-}$ mice compared with WT mice (Fig. 5*B*). To investigate LXR regulation of glucose uptake in BAT further, staining of Glut4 was performed. A more intense GLUT4-positive reaction was observed in the BAT of LXRα$^{-/-}$ as well as LXRβ$^{-/-}$ mice (Fig. 5*C*) compared with WT animals as confirmed by Western blot analysis, wherein a sixfold and 3.8-fold increase of GLUT4 expression was observed in LXRα$^{-/-}$ and LXRβ$^{-/-}$ mice, respectively, compared with WT animals (Fig. 5*D*). In addition, GW3965 chronic treatment included in the diet induced a 4.5-fold increase of GLUT4 expression in WT mice with no effect in LXRα$^{-/-}$ and LXRβ$^{-/-}$ mice.

Regulation of Brown Fat-Selective Genes and Fat Storage by LXRs. To investigate the role of LXRα and LXRβ in the regulation of EE and lipid metabolism in BAT further, mRNA expression of well-known genes involved in these regulations was measured in WT, LXRα$^{-/-}$, and LXRβ$^{-/-}$ mice on the ND (Fig. 6). All analyzed genes [*cell death activator* (*CIDEA*), *deiodinase iodothyronine type II* (*Dio2*), and *Leptin*) were up-regulated in LXRα$^{-/-}$ and LXRβ$^{-/-}$ mice compared with WT mice, except for *Leptin*, which was down-regulated in LXRβ$^{-/-}$ mice compared with WT mice (Fig. 6*A*, *Top*). It is well accepted that to increase nonshivering thermogenesis, both UCP1 transcription and activation have to be fortified. We thus analyzed well-known target genes involved in these two pathways. BAT thermogenesis is activated through adrenergic receptor (AR) activation by norepinephrine release

PHYSIOLOGY

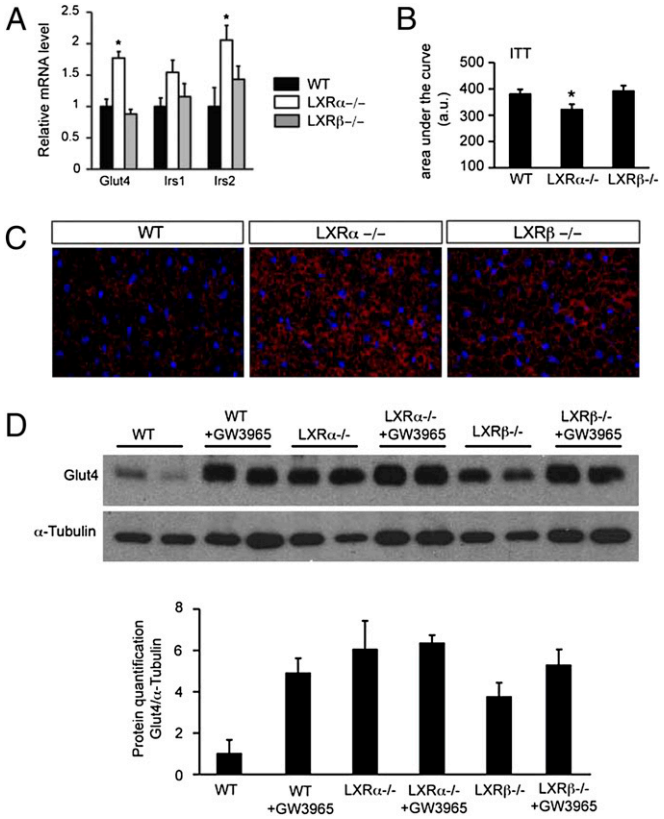

Fig. 5. LXRs regulate GLUT4 in BAT. (*A*) mRNA expression levels of genes involved in glucose regulation in the BAT of WT (black bar), LXRα$^{-/-}$ (white bar), and LXRβ$^{-/-}$ (gray bar) mice respectively, on the ND. Relative fold changes in expression levels were compared with WT mice, in which the expression was set to 1.0 and normalized to TFIID expression (one-way ANOVA, n = 5–7 animals per group; *$P < 0.05$ in LXR KO vs. WT mice). (*B*) Area under the curve of peripheral glucose output following an i.p. insulin injection in WT, LXRα$^{-/-}$, and LXRβ$^{-/-}$ mice (two-tailed t test, n = 7 animals per group; *$P < 0.05$ in LXR KO vs. WT mice). (*C*) One representative immunofluorescence study of GLUT4 in the BAT of WT, LXRα$^{-/-}$, and LXRβ$^{-/-}$ mice on the ND. (*D*) Detection of GLUT4 expression in BAT by Western blotting in WT, LXRα$^{-/-}$, and LXRβ$^{-/-}$ mice on ND ± GW3965-fed mice.

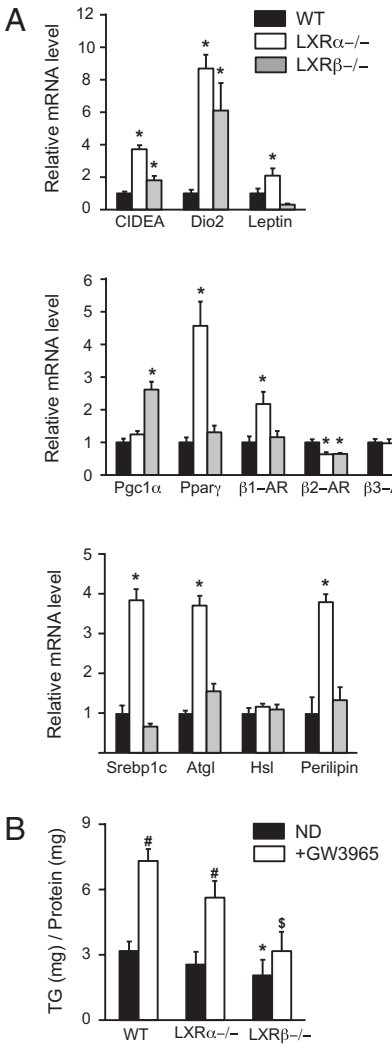

Fig. 6. LXRs regulate fat storage and brown fat-selective genes in BAT. (*A*) mRNA expression levels of genes involved in the regulation of energy metabolism, the thermogenesis pathway, and lipid metabolism in the BAT of WT (black bar), LXRα$^{-/-}$ (white bar), and LXRβ$^{-/-}$ (gray bar) mice, respectively, on the ND. Relative fold changes in expression levels were compared with WT mice, in which the expression was set to 1.0 and normalized to TFIID expression (one-way ANOVA, n = 5–7 animals per group). (*B*) TG content in the BAT of WT, LXRα$^{-/-}$, and LXRβ$^{-/-}$ mice on the ND (black bar) and ND + GW3965 (white bar), respectively (two-tailed t test, n = 5–8 animals per group; *$P < 0.05$ in LXR KO vs. WT mice; $^{\#}P < 0.05$ in ND vs. ND + GW3965 mice; $^{\$}$LXR KO ND + GW3965 vs. WT ND + GW3965 mice).

from sympathetic nerves. Surprisingly, mRNA level of *β2-AR* was lower in both genotypes, whereas expression of the *β3-AR* gene was significantly decreased in LXRβ$^{-/-}$ mice compared with WT animals (Fig. 6*A*, *Middle*). LXRβ$^{-/-}$ but not LXRα$^{-/-}$ mice showed increased *peroxisome proliferator-activated receptor γ coactivator 1α* (*PGC1α*) expression compared with WT mice. Conversely, expression of *Pparγ* and *β1-AR* was up-regulated in LXRα$^{-/-}$ compared with WT animals (Fig. 6*A*, *Middle*). One pathway of UCP1 activation is through hormone-sensitive lipase (*Hsl*), a rate-limiting enzyme in lipolysis (29). We found no differences between the three genotypes in *Hsl* expression level. Nevertheless, expression of both *adipose triglyceride lipase* (*Atgl*) and *perilipin α* (*Plin1*) in LXRα$^{-/-}$ mice and of *Plin1* only in LXRβ$^{-/-}$ mice, two well-known regulators of lipolysis, was up-regulated compared with that in WT animals (Fig. 6*A*, *Bottom*). Finally, expression of *sterol regulatory binding transcription factor 1* (*Srebp1c*), a key regulator of lipogenesis, was fourfold higher in LXRα$^{-/-}$ mice but not in LXRβ$^{-/-}$ mice compared with WT mice (Fig. 6*A*, *Bottom*). This result indicates that LXRα may act as a repressor of lipogenesis in BAT, a completely opposite response to the one observed in the liver. To investigate the role of LXRs in lipid accumulation in BAT further, we quantified triglyceride (TG) content in the BAT of WT, LXRα$^{-/-}$, and LXRβ$^{-/-}$ mice on the ND in the presence or absence of GW3965 (Fig. 6*B*). The TG content was significantly lower in LXRβ$^{-/-}$ mice compared with WT on the ND in both the presence and absence of GW3965, whereas no differences were observed between LXRα$^{-/-}$ and WT mice. Addition of long-term GW3965 to the diet induced TG accumulation (twice) in the BAT of WT and LXRα$^{-/-}$ mice but not in LXRβ$^{-/-}$ mice, suggesting a regulation of fat storage through LXRβ in BAT, another mechanism by which LXRβ may regulate EE in BAT.

Discussion

It has long been recognized that LXRs regulate energy metabolism as well as glucose and fat metabolism (16–18, 30, 31). As opposed to the study of Wang et al. (20), in the present study, we present evidence that LXRα as well as LXRβ regulates EE through UCP1 expression in mouse BAT. Indeed, although the

absence of both LXRα and LXRβ leads to increased EE and increased UCP1 expression, chronic stimulation of LXR with GW3965 ligand showed reduced EE in female mice as well as reduced UCP1 expression in the BAT of WT, LXRα$^{-/-}$, and LXRβ$^{-/-}$ mice. This is in accordance with previously published data from Stulnig et al. (32) showing that LXR agonist treatment for 5 d leads to a 2.4-fold decrease of UCP1 expression in mouse BAT. Both transcription and activation of UCP1 are required for increased BAT thermogenesis. In this study, we suggest that two different mechanisms lead to UCP1 activation through LXRs in BAT. When LXRβ is absent, UCP1 transcription may be activated through an increase of *Pgc1α* expression, and when LXRα is absent, UCP1 transcription may be activated through up-regulation of *Pparγ* expression (Fig. 6*A*). Cross-talk between PPAR and LXR transcription factors has been proposed by Ide et al. (33) and Yoshikawa et al. (34), who suggested that these two nuclear receptors could interfere with each other's ability to activate target genes by competing for limited amounts of retinoid-X receptor. In addition, Wang et al. (20) supported such interaction in a brown adipose cell line. In our study, a competition between LXRs and PPAR at the UCP promoter level could explain the observed repression of UCP expression under chronic GW3965 treatment in WT and LXRα$^{-/-}$ mice (Fig. 4*D*).

Moreover, in the current study, only β1-AR gene expression but not β3-AR expression was significantly up-regulated in LXRα$^{-/-}$ but not LXRβ$^{-/-}$ mice compared with WT mice. β1 stimulation is a well-established pathway of brown preadipocyte proliferation (35, 36), whereas functional β3-AR is not found in brown preadipocytes (37). These data support the idea of LXRα as a regulator of brown preadipocyte proliferation to regulate EE. In addition, LXRα$^{-/-}$ mice showed increased expression levels of genes involved in energy metabolism as well as lipid metabolism. Leptin expression level in the BAT of LXRα$^{-/-}$ mice was 100% higher than in WT animals as opposed to LXRβ$^{-/-}$ mice, in which leptin expression was 70% lower than in WT animals. Most studies converge to say that total BAT activity is inversely associated with adiposity, suggesting that increasing BAT mass and/or activity may be an aim for pharmaceutical intervention to treat obesity. In the current study, whole-body fat content measured by MRI showed less TF in LXRβ$^{-/-}$ mice but not in LXRα$^{-/-}$ mice on the ND compared with WT mice (Fig. 3*A*). We have previously shown that LXRαβ$^{-/-}$ and LXRβ$^{-/-}$ mice but not LXRα$^{-/-}$ mice were protected against diet-induced obesity (18). In this respect, the mechanisms by which LXRα$^{-/-}$ mice showed similar fat content but higher UCP1 expression in both SC fat and BAT than WT mice on the ND remain unclear and have to be investigated further. In this respect, increased UCP1 expression in BAT and gonadal fat cannot be correlated to a decrease of fat mass.

The UCP1-ablated mice, surprisingly, are resistant to diet-induced obesity when housed at 23 °C (38) but not when housed at thermoneutrality (30 °C) (39). In the current study, a trend toward increased EE was observed in LXRαβ$^{-/-}$ mice compared with WT mice when monitored at 30 °C for 3 h (Fig. 1*B*). In addition, when WT mice were chronically treated with LXR ligand (GW3965) for 3 wk, EE was significantly lower than in nontreated WT mice at 30 °C. These data from in vivo experiments would suggest a mechanism other than UCP1 activation by which LXR regulates EE. Indeed, it is well established that under conditions in which sympathetic nervous system activity is minimized (thermoneutrality), BAT loses the feature of UCP1-dependent thermogenesis (11). Recent research has indicated, for reasons that are not fully understood, that mammals may demonstrate a type of thermogenesis that is also brown fat-associated, even in the absence of any need for thermoregulatory thermogenesis (11), so-called "metaboloregulatory thermogenesis." The observed GLUT4 overexpression in the BAT of LXRα$^{-/-}$ and LXRβ$^{-/-}$ mice might be one potential mechanism of metaboloregulatory thermogenesis to reduce fat storage. Conversely, EE was doubled in LXRαβ$^{-/-}$ mice when monitored at 4 °C compared with WT mice. These data strongly support UCP1 regulation of EE by LXRs in the conditions of stimulated nonshivering thermogenesis. Surprisingly, LXRαβ$^{-/-}$ and LXRβ$^{-/-}$ mice but not LXRα$^{-/-}$ mice have been shown to be resistant to diet-induced obesity (17, 18, 22). This is in conflict with the findings of Wang et al. (20), who concluded that LXRα$^{-/-}$ mice have increased mitochondria and ectopic UCP1 expression in WAT that might protect these animals from diet-induced obesity. These authors conclude that LXRα is the operational isoform responsible for increased basal UCP1 expression and mitochondrial biogenesis (20). Our results would suggest a mechanism other than increased UCP1 thermogenesis by which LXRβ$^{-/-}$ mice increase EE and are protected from high-fat diet-induced obesity, as already shown (18). LXRβ is the main isoform in the muscle tissue; one possibility could be that LXRβ regulates thermogenesis in the muscle tissue to protect mice against diet-induced obesity. This hypothesis has to be addressed in future experiments and would involve tissue-specific ablation of the LXR isoforms.

Finally, it is well known that thyroid hormone increases thermogenesis and UCP1 expression in BAT (40, 41). Recently, Christoffolete et al. (42) showed that LXR stimulation negatively regulates *Dio2* transcription in human liver. In our study, *Dio2* expression is sixfold and eightfold higher in LXRα$^{-/-}$ and LXRβ$^{-/-}$ mice, respectively, compared with WT mice. Thus, this is another pathway by which LXRs could regulate EE, but the exact mechanism remains unclear.

The pharmacological approach to treat obesity by increasing EE through thermogenesis has already proved to be effective in weight loss (3, 4, 11). In the current study, we have shown that the regulation of LXR activity in BAT could be a potential target for controlling EE and weight loss.

Experimental Procedures

Animals. Ten-week-old female C57BL/6 WT and LXRα and LXRβ KO mice [as previously described (43)] were housed on a regular 12-h light/12-h dark cycle with free access to water and food unless otherwise specified. Mice were fed for 3 wk either an ND containing 4% (wt/wt) total lipids (<12% of its calories as animal fat) and <0.04% (wt/wt) cholesterol (TD 7001; Harlan Teklad) or an HCD containing 70.4% (wt/wt) total carbohydrate (64.5% from sucrose) and 11.8% (wt/wt) fat (TD 98090; Harlan Teklad), and GW3965 (0.025%, 250-mg/kg diet; GlaxoSmith) was mixed to the diet or given by gavage for 3 d (50 mg/kg) when specified. BW was recorded at day 0 and every 3 d after the beginning of the diet period. Food consumption was measured for 8 consecutive days in the middle of the diet period. The energy content of the food ingested was calculated based on information from the manufacturers of the food. All experiments were approved by the local ethical committee on animal research.

Energy Consumption. Mice were individually housed in calorimeter cages and acclimatized to the chamber for 2 d before gas exchange measurements. Indirect calorimetry was performed using a computer-controlled SOMEDIC Metabolic system-INCA (SOMEDIC Sales AB). Oxygen consumption and carbon dioxide production were measured for each mouse at 20-min intervals over a 48-h period. EE, glucose oxidation, and lipid oxidation were calculated as previously described (18). Measurements were performed during the 12-h light/12-h dark cycle at 23 °C with full access to food and water. Between 6:00 and 9:00 AM, the cage temperature was decreased down to 4 °C on day 1 and increased to 30 °C on day 2.

i.p. Insulin Tolerance Tests. Mice were fasted ~4 h before testing. Insulin (0.8 U/kg, Actrapid Penfill; NovoNordisk) was injected i.p., and glucose was measured with the OneTouch Ultra glucometer (Accu-Chek Sensor; Roche Diagnostics) as previously described (18).

In Vivo MRI. In vivo MRI fat distribution was measured in every mouse within 1 wk after the 3-wk diet period. All measurements were performed as previously described (18). The abdominal fat is the sum of VS and SC fat within the abdominal region. MRI-visible VS fat comprises gonadal, omental, peritoneal, and retroperitoneal fat depots.

Chemical Analysis of Tissue. At the end of the experiment, animals were killed and interscapular BAT was quickly collected and frozen in liquid nitrogen for further analysis. Brown adipose lipids were extracted according to Folch et al. (44). TG was measured by enzymatic assay using commercial kits (Roche Diagnostics).

Histology of BAT. The interscapular BAT was removed and fixed overnight in 4% (wt/vol) paraformaldehyde at 4 °C and embedded in paraffin. Sections (4-μm thickness) were stained with H&E according to standard histological procedures.

Immunohistochemical Staining. Representative blocks of paraffin-embedded tissues were cut at a thickness of 4 μm, dewaxed, and rehydrated. For UCP1, sections were first incubated in 0.5% H_2O_2 in PBS for 30 min at room temperature to quench endogenous peroxidase. Afterward, sections (UCP1 and GLUT4) were incubated in 0.5% Triton X-100 in PBS for 30 min. To block nonspecific binding, sections were incubated in 3% (wt/vol) BSA for 1 h at 4 °C. Sections were incubated with anti-UCP1 or anti-GLUT4 antibody at a dilution of 1:200 in 1% BSA and 0.1% P40 in PBS overnight at 4 °C. BSA replaced primary antibodies in negative controls. After washing, sections were incubated with the corresponding secondary antibodies (1:200 dilution) for 2 h at room temperature. For UCP1, sections were lightly counterstained with hematoxylin, dehydrated through an ethanol series to xylene, and mounted. For GLUT4, sections were counterstained with DAPI and directly mounted in Vectashield antifading medium (Vector Laboratories). UCP1- and GLUT4-stained sections were examined under a light microscope or a Zeiss fluorescence microscope with filters suitable for selectively detecting the fluorescence of FITC (green) and Cy3 (red), respectively.

Western Blotting. Fifty micrograms of total cellular protein was separated on 4–10% Tris_Glycine Gel kit (Invitrogen). The following primary antibodies were used: anti-UCP1 (M-17, sc 6529; Santa Cruz), anti-glut4 (Ab654-250; Abcam), and anti–α-tubulin (11H10, 2125s; Cell Signaling). Secondary antibodies were HRP-conjugated anti-goat and anti-rabbit (Sigma). Visualization was carried out using ECL plus (Amersham). Protein levels were normalized to tubulin expression.

Quantitative PCR. RNA was extracted using TRIzol according to the manufacturer's instructions (Invitrogen AB). mRNA expression levels were quantified using an ABI 7500 instrument and SYBR green technology (Applied Biosystems). Relative gene expression changes were calculated with the comparative C_T method using TFIID as an internal reference gene.

Statistics. All values are expressed as means ± SEM. Differences between groups or diets were determined by a two-tailed Student's *t* test or one-way ANOVA as indicated for specific experiments in the figure legends. The Tukey post hoc test was used to identify the location of significant differences when appropriate. The level of significance was set at $P < 0.05$.

ACKNOWLEDGMENTS. We thank Lilian Larsson and Christina Thulin-Anderson for excellent technical help. This work was supported by the Swedish Science Council, the Robert A. Welch Foundation, the European Union Integrated Project Coordination Action on Risks, Evolution of Threats and Context Assessment by an Enlarged Network for an R&D Roadmap (CRESCENDO), and Emil and Wera Cornells Stiftelse.

1. Cannon B, Nedergaard J (2010) Metabolic consequences of the presence or absence of the thermogenic capacity of brown adipose tissue in mice (and probably in humans). *Int J Obes (Lond)* 34(Suppl 1):S7–S16.
2. Nedergaard J, Cannon B (2010) The changed metabolic world with human brown adipose tissue: Therapeutic visions. *Cell Metab* 11:268–272.
3. Cannon B, Nedergaard J (2004) Brown adipose tissue: Function and physiological significance. *Physiol Rev* 84:277–359.
4. Hansen JB, Kristiansen K (2006) Regulatory circuits controlling white versus brown adipocyte differentiation. *Biochem J* 398:153–168.
5. Smith RE, Horwitz BA (1969) Brown fat and thermogenesis. *Physiol Rev* 49:330–425.
6. Trayhurn P (1995) Fuel selection in brown adipose tissue. *Proc Nutr Soc* 54:39–47.
7. Trayhurn P, Duncan JS, Rayner DV (1995) Acute cold-induced suppression of ob (obese) gene expression in white adipose tissue of mice: Mediation by the sympathetic system. *Biochem J* 311:729–733.
8. Cypess AM, Kahn CR (2010) The role and importance of brown adipose tissue in energy homeostasis. *Curr Opin Pediatr* 22:478–484.
9. Cypess AM, Kahn CR (2010) Brown fat as a therapy for obesity and diabetes. *Curr Opin Endocrinol Diabetes Obes* 17:143–149.
10. Tseng YH, Cypess AM, Kahn CR (2010) Cellular bioenergetics as a target for obesity therapy. *Nat Rev Drug Discov* 9:465–482.
11. Cannon B, Nedergaard J (2009) Thermogenesis challenges the adipostat hypothesis for body-weight control. *Proc Nutr Soc* 68:401–407.
12. Nedergaard J, Bengtsson T, Cannon B (2007) Unexpected evidence for active brown adipose tissue in adult humans. *Am J Physiol Endocrinol Metab* 293:E444–E452.
13. Valverde AM, Benito M, Lorenzo M (2005) The brown adipose cell: A model for understanding the molecular mechanisms of insulin resistance. *Acta Physiol Scand* 183:59–73.
14. Escher P, et al. (2001) Rat PPARs: Quantitative analysis in adult rat tissues and regulation in fasting and refeeding. *Endocrinology* 142:4195–4202.
15. Steffensen KR, et al. (2003) Gene expression profiling in adipose tissue indicates different transcriptional mechanisms of liver X receptors alpha and beta, respectively. *Biochem Biophys Res Commun* 310:589–593.
16. Anthonisen EH, et al. (2010) Nuclear receptor liver X receptor is O-GlcNAc-modified in response to glucose. *J Biol Chem* 285:1607–1615.
17. Kalaany NY, et al. (2005) LXRs regulate the balance between fat storage and oxidation. *Cell Metab* 1:231–244.
18. Korach-André M, et al. (2010) Separate and overlapping metabolic functions of LXRalpha and LXRbeta in C57Bl/6 female mice. *Am J Physiol Endocrinol Metab* 298: E167–E178.
19. Mitro N, et al. (2007) The nuclear receptor LXR is a glucose sensor. *Nature* 445:219–223.
20. Wang H, et al. (2008) Liver X receptor alpha is a transcriptional repressor of the uncoupling protein 1 gene and the brown fat phenotype. *Mol Cell Biol* 28:2187–2200.
21. Gabbi C, et al. (2008) Pancreatic exocrine insufficiency in LXRbeta−/− mice is associated with a reduction in aquaporin-1 expression. *Proc Natl Acad Sci USA* 105: 15052–15057.
22. Gerin I, et al. (2005) LXRbeta is required for adipocyte growth, glucose homeostasis, and beta cell function. *J Biol Chem* 280:23024–23031.
23. Rothwell NJ, Stock MJ (1983) Diet-induced thermogenesis. *Adv Nutr Res* 5:201–220.
24. Collins JL, et al. (2002) Identification of a nonsteroidal liver X receptor agonist through parallel array synthesis of tertiary amines. *J Med Chem* 45:1963–1966.
25. Kajimura S, Seale P, Spiegelman BM (2010) Transcriptional control of brown fat development. *Cell Metab* 11:257–262.
26. Cannon B, Shabalina IG, Kramarova TV, Petrovic N, Nedergaard J (2006) Uncoupling proteins: A role in protection against reactive oxygen species—or not? *Biochim Biophys Acta* 1757:449–458.
27. Nikami H, Shimizu Y, Endoh D, Yano H, Saito M (1992) Cold exposure increases glucose utilization and glucose transporter expression in brown adipose tissue. *Biochem Biophys Res Commun* 185:1078–1082.
28. Slot JW, Geuze HJ, Gigengack S, Lienhard GE, James DE (1991) Immuno-localization of the insulin regulatable glucose transporter in brown adipose tissue of the rat. *J Cell Biol* 113:123–135.
29. Sell H, Deshaies Y, Richard D (2004) The brown adipocyte: update on its metabolic role. *Int J Biochem Cell Biol* 36:2098–2104.
30. Janowski BA, Willy PJ, Devi TR, Falck JR, Mangelsdorf DJ (1996) An oxysterol signalling pathway mediated by the nuclear receptor LXR alpha. *Nature* 383:728–731.
31. Schultz JR, et al. (2000) Role of LXRs in control of lipogenesis. *Genes Dev* 14: 2831–2838.
32. Stulnig TM, et al. (2002) Novel roles of liver X receptors exposed by gene expression profiling in liver and adipose tissue. *Mol Pharmacol* 62:1299–1305.
33. Ide T, et al. (2003) Cross-talk between peroxisome proliferator-activated receptor (PPAR) alpha and liver X receptor (LXR) in nutritional regulation of fatty acid metabolism. II. LXRs suppress lipid degradation gene promoters through inhibition of PPAR signaling. *Molecular Endocrinol* 17:1255–1267.
34. Yoshikawa T, et al. (2003) Cross-talk between peroxisome proliferator-activated receptor (PPAR) alpha and liver X receptor (LXR) in nutritional regulation of fatty acid metabolism. I. PPARs suppress sterol regulatory element binding protein-1c promoter through inhibition of LXR signaling. *Molecular Endocrinol* 17:1240–1254.
35. Géloën A, Collet AJ, Guay G, Bukowiecki LJ (1988) Beta-adrenergic stimulation of brown adipocyte proliferation. *Am J Physiol* 254:C175–C182.
36. Rehnmark S, Nedergaard J (1989) DNA synthesis in mouse brown adipose tissue is under beta-adrenergic control. *Exp Cell Res* 180:574–579.
37. Bronnikov G, et al. (1999) beta1 to beta3 switch in control of cyclic adenosine monophosphate during brown adipocyte development explains distinct beta-adrenoceptor subtype mediation of proliferation and differentiation. *Endocrinology* 140:4185–4197.
38. Enerbäck S, et al. (1997) Mice lacking mitochondrial uncoupling protein are cold-sensitive but not obese. *Nature* 387:90–94.
39. Feldmann HM, Golozoubova V, Cannon B, Nedergaard J (2009) UCP1 ablation induces obesity and abolishes diet-induced thermogenesis in mice exempt from thermal stress by living at thermoneutrality. *Cell Metab* 9:203–209.
40. Silva JE, Bianco SD (2008) Thyroid-adrenergic interactions: Physiological and clinical implications. *Thyroid* 18:157–165.
41. Silva JE (2006) Thermogenic mechanisms and their hormonal regulation. *Physiol Rev* 86:435–464.
42. Christoffolete MA, et al. (2010) Regulation of thyroid hormone activation via the liver X-receptor/retinoid X-receptor pathway. *J Endocrinol* 205:179–186.
43. Alberti S, et al. (2001) Hepatic cholesterol metabolism and resistance to dietary cholesterol in LXRbeta-deficient mice. *J Clin Invest* 107:565–573.
44. Folch J, Lees M, Sloane Stanley GH (1957) A simple method for the isolation and purification of total lipides from animal tissues. *J Biol Chem* 226:497–509.